Sex-Dependent Effects of Chronic Stress During Adolescence on Cognitive Bias and Functional Connectome in Young Adult Rats

Twain Dai[1,2*], Liz Jaeschke-Angi[1,2], Marissa Penrose-Menz[1,2], Tim Rosenow[3], Jennifer Rodger[1,2]

[1]School of Biological Sciences, The University of Western Australia, Perth, WA, Australia

[2]Perron Institute for Neurological and Translational Sciences, The University of Western Australia, Perth, WA, Australia

[3]Centre for Microscopy, Characterisation & Analysis, Research Infrastructure Centres, The University of Western Australia, 6009 Western Australia, Australia

*** Correspondence:**

Twain Dai

twain.dai@research.uwa.edu.au

Six keywords: Resting-State Functional MRI, Chronic Restraint Stress, Judgement Bias, Open Field Test, Sex Differences

Word Counts: 4287

Abstract

Negative cognitive biases in depression are more pronounced in females than in males. This sex difference emerges during adolescence, a sensitive developmental stage when chronic stress exposure increases the risk of depression in adulthood. The neurobiology linking adolescent stress to sex-specific cognitive bias and resting-state network reorganization in adults remain poorly understood. The study aimed to investigate the longitudinal effects of chronic restraint stress (CRS) during adolescence on cognitive bias and functional connectome in emerging adulthood. 28 Wistar rats (sex-balanced; aged five weeks on arrival) were trained on a judgment bias task with distinct tactile cues signalling differential rewards. Cognitive bias was quantified from responses to ambiguous probe trials. Following training, animals were randomly and equally assigned to CRS or control groups (sex-balanced). Offline resting-state functional MRI scans were conducted at adolescent baseline (pre-CRS) and again in adulthood (post-CRS), followed by probe trials to assess neural and behavioural changes. Following CRS, females showed a greater tendency to shift toward negative bias than males (ratio of odds ratio=3.67). Furthermore, CRS significantly reduced functional connectivity between the left cerebellar–auditory and hypothalamic–thalamic networks only in females. Repeated-measures correlation between cognitive bias and network connectivity were not statistically significant across sex-by-group strata, potentially due to offline imaging and small sample size. However, intra-individual association revealed sex-specific trends, with CRS females showing moderately positive correlations and CRS males exhibiting a weak negative association. The results could inform stratified connectome-based interventions targeting adolescent stress exposures to potentially reduce the risk of adult depression.

Introduction

Adolescence is a critical developmental period during which the brain undergoes profound structural and functional refinements, particularly cortical-subcortical circuits that govern stress regulation and cognitive processing (1, 2). Recent large-scale connectomics studies reveal that different neural circuits undergo heterochronic refinement during the transition to adulthood (3, 4). While primary sensory-motor circuits reach functional stability in early childhood, higher-order affective and cognitive networks experience ongoing refinement throughout adolescence. This developmental mismatch highlights adolescence as a pivotal turning point where functional organization of the brain is uniquely sensitive to environmental adversities (5).

Chronic exposure to stressful events during adolescence is known to derail these developmental trajectories by disrupting the normative refinement of cortical-subcortical circuits, significantly increasing the risk of depression in adulthood (6). The resulting psychiatric vulnerability is behaviourally characterized by negative cognitive biases, a systematic tendency to prioritize the processing of aversive information over neutral or positive stimuli (7). These biases are not merely symptoms of affective dysfunction but are considered core factors that predict the onset and chronicity of depression (8, 9). This predictive relationship is notably stronger in females. Longitudinal behavioural evidence demonstrates that the interaction between negative cognitive biases and stress more robustly affects depression trajectories in females than in males during adolescence (10).

The sex difference in negative cognitive biases is mirrored by distinct neural signatures. Specifically, adolescent females with depression exhibit unique recruitment of the posterior cingulate and supramarginal gyrus when faced with negative distractors, a response absent in their male counterparts (11). Furthermore, the neural correlates of cognitive bias are divergent during memory processing: while adolescent females with depression exhibit amygdala hyperactivity during negative recall, male counterparts are characterized by reduced hippocampal engagement during positive recall (12). Although human neuroimaging studies demonstrate correlation between sex-specific biases in depression and aberrant connectivity, a causal understanding of how adolescent chronic stress sculpts the resting-state reorganization to lock in sex-specific cognitive biases in adulthood remains elusive. Gaining a deeper understanding of these mechanisms could inform novel, targeted strategies for preventing adult depression.

Rodent models offer unique advantages to study neurobiology and enable hypothesis testing that is not feasible in humans, including the induction of chronic stress under highly controlled conditions (13, 14). Specifically, chronic stress in adolescent rodents induces detrimental effects on affective behaviours in adulthood (15, 16). Similar to humans, a key manifestation is a shift toward pessimistic judgment bias, which can be objectively quantified using translational paradigms such as the judgment bias task (JBT). By measuring how animals interpret ambiguous cues to assess levels of optimism and pessimism, the JBT has demonstrated that adolescent stress induces a persistent pessimistic bias, mirroring the negative cognitive bias of human

depression (17, 18). However, most preclinical research continues to prioritize males, leaving the neural mechanisms driving female-specific cognitive biases following chronic stress largely unexplored (19, 20). This knowledge gap is further magnified by a lack of longitudinal data mapping the sex-specific developmental trajectory of neural network as it unfolds from adolescent stress exposure through to adulthood (15).

Therefore, this study employed a longitudinal design to bridge the gap between cognitive bias and whole-brain resting-state functional architecture within the same cohort of males and females before and after adolescent chronic stress. The study aimed to map the sex-specific trajectories of resting-state network refinement and judgement bias following adolescent chronic stress, identifying the neural signatures that characterize the transition into an adult “pessimistic” state in a rodent model.

Methods

Ethics Statement

Ethical approvals for the animal experiment (2023/ET000552) were obtained from the animal ethics committee of the University of Western Australia (UWA).

Animals and Study Design

28 Wistar rats (14 females/14 males; aged 5 weeks and weighing 110 ~ 200 g on arrival) were sourced from the Ozgene Animal Resources Centre, Western Australia. All rats were housed under a reverse 12-hour light-dark cycle with ad libitum food and water, in a temperature-controlled room located at UWA's Animal Care Unit (Nedlands, WA). Rats aged 55 ~ 70 days were categorized as adolescents, whereas those aged 70 ~ 150 days were considered emerging adults (21). While the oestrous cycle was not explicitly tracked, the longitudinal nature of behavioural task and the focus on resting-state connectome reorganization likely mitigated the influence of acute hormonal fluctuations on primary outcomes. All animals (housed in pairs) were acclimatized to the new environment and handled for nine days after their arrival and prior to experiments.

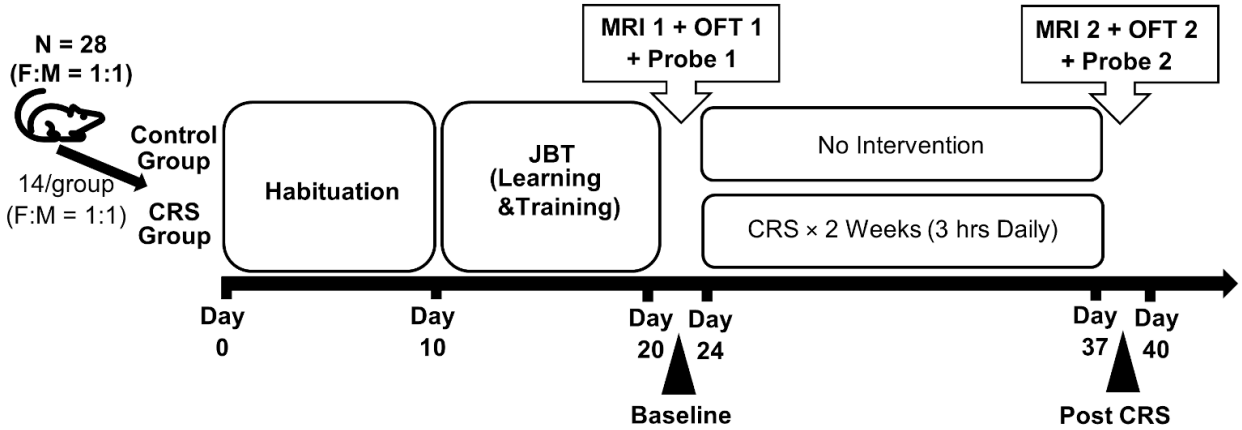

Figure 1. Study Design and Timeline. All animals were habituated to the new environment for nine days after their arrival and prior to experiments. All rats were trained on JBT, for up to nine days. Behavioural tests and MRI scan were conducted before and after 14 consecutive days of CRS.

Animals were randomly and equally assigned to two sex-balanced groups: control (7 females/7 males) and CRS groups (7 females/7 males). On Day 9 after their arrival, animals began single-housed and mild food restrictions overnight, with food pellets removed at 4 pm. From Day 10 onward, animals were trained on the JBT (*Figure 1*). Animals remained under mild food restrictions, with two hours of free access to food each day until pre-probe was completed. Animals were excluded from further experiments if they did not successfully complete JBT training within nine days. Once an animal was verified to have learned the task through the pre-probe test, it underwent a pre-OFT, which habituates rats to the testing arena. Following the pre-OFT, animals received no intervention until Day 21. Baseline MRI scan, OFT and JBT probe for all animals were conducted on Day 21, 22 and 23, respectively. From Day 24 onwards, animals in the CRS group underwent CRS for 14 consecutive days. The second MRI scan, OFT and JBT probe for all rats

were carried out on Day 38, 39, and 40, respectively. For the baseline and post-CRS probes, food was removed overnight starting at 4 pm on Day 22 and 39, respectively.

Judgment Bias Task

Task Design

The JBT in the present study was Go/Go task and adapted from Brydges and Hall (22). The task required animal's responses to different tactile stimuli, olfactory and spatial cues, which were associated with different reward values. The task involved two reward values (large and small), two distinct tactile stimuli (coarse and fine), two distinct olfactory cues (cinnamon and coriander) and two distinct spatial cues (left and right), resulting in eight task combinations *(Supplementary Table 1)*. The assignment of task combinations was randomized equally across animals in each sex group and remained consistent for each animal throughout the experiment. The olfactory and location cues were employed to accelerate memory formation in learning the association between tactile stimuli and reward values.

Apparatus

The JBT apparatus (*Figure 2A*) was custom-built from acrylic in tint gray (The Plastic People, Osborne Park, WA). It consisted of three compartments: one start compartment (50 cm length × 50 cm width × 60 cm height) and two reward compartments (30 cm length × 15 cm width × 60 cm height). One removable barrier separated the start compartment from the reward compartments. A sandpaper (tactile stimuli) was attached to the centre of the start compartment using Velcro tapes when required. One ceramic foraging bowl containing cheerios (rewards) was placed at the end of each reward compartment. One small muslin bag containing coriander or cinnamon was hung on each sidewall of each reward compartment.

Procedures and Bias Measures

The JBT consisted of four phases: spatial and olfactory learning, tactile learning, training, and probe phases (*Figure 2*).

During the spatial and olfactory learning phase, animals were trained to learn the assigned association among reward values, spatial and olfactory cues. Different amounts of cheerios (rewards) were placed in two reward compartments. Animals were free to retrieve rewards from both compartments. This phase was considered complete when animals retrieved rewards from each compartment 5 times. Animals then proceeded to tactile learning the following day.

During the tactile learning phase, animals were further trained to learn the assigned association between reward values and tactile stimuli, in addition to the spatial and olfactory cues. Animals had free access to both reward compartments for a total of 30 trials. In each trial, only one compartment was baited, and a coarse (P60) or fine (P1500) sandpaper was secured to the floor in the centre of the start compartment. The high and low reward trials were randomly assigned, with the rule that no more than two trials in a row were assigned the same size of reward. When animals completed 90% (27/30) of the trials within an hour, they proceeded to the training phase the following day.

The training phase was identical to the tactile learning phase, except that animals were only allowed to enter one reward compartment of their choice and prevented from entering the other reward compartment by placing an acrylic barrier following their choice. In addition, in one in every five trials, no reward was initially placed in either reward compartment; but animals were awarded a corresponding size of reward immediately after making the right choice, while no reward was given for an incorrect choice. This controlled any olfactory cues from cheerios that might guide decision-making and also served as reinforcement to enhance learning and reduce extinction. The training phase consisted of up to three training sessions in a day, with each training session containing 16 trials. Training continued until animals achieved 75% (12/16) accuracy in a training session.

All male rats (N = 14) completed the learning and training phases within four days, except for one that spent five days. Conversely, female rats (N = 12) took longer, with durations ranging from four to nine days. Two female rats did not complete the learning and training phases within nine days and were excluded from further experiments (Final N = 26; 12 females/14 males).

Following the completion of training, animals underwent one pre-probe, one baseline probe, and one post-CRS probe. The pre-probe was conducted the day after training was completed to verify that animals had learned assigned task combination. Baseline and post-CRS probes were carried out on Day 23 and 40, respectively. The probe phase was similar to the training phase, except that there were a total of 30 trials and one in every five trials was unrewarded. In these six unrewarded trials, three intermediate and ambiguous grades of sandpaper (P240, P320, P400) were randomly assigned and each presented twice as probes. The random presentation of three ambiguous tactile stimuli aimed to ensure that the animals did not learn that there were no rewards in ambiguous trials and always chose a reward compartment. Judgement bias was assessed using response data from six ambiguous trials in the probe session that met the completion criteria, on an integer scale ranging from -3 to 3. A score of 3 represented an extremely positive bias, characterized by six high-reward responses; a score of 0 suggested a neutral bias, characterized by equal high-reward and low reward responses; whereas a score of -3 indicated an extremely negative bias, characterized by six low-reward responses.

Chronic Restraint Stress

From Day 24 to Day 37, CRS was performed on a bench situated in one corner of a spacious animal holding room, with rats in the intervention group (6 females/7 males) placed in a transparent plastic tube facing the wall to mitigate visual distractions (23). Each session started between 12:00 and 13:00 PM, lasting for three hours daily to reduce the influence of circadian rhythm. Following each session, animals were immediately returned to their home cages. The control group (6 females/7 males) stayed in their home cages without undergoing CRS.

Open Field Test and Behavioural Automation

OFT (24) was conducted in an open arena (50 cm length × 50 cm width × 60 cm height) to evaluate anxiety-like behaviours, with each animal tested individually. Animals were positioned

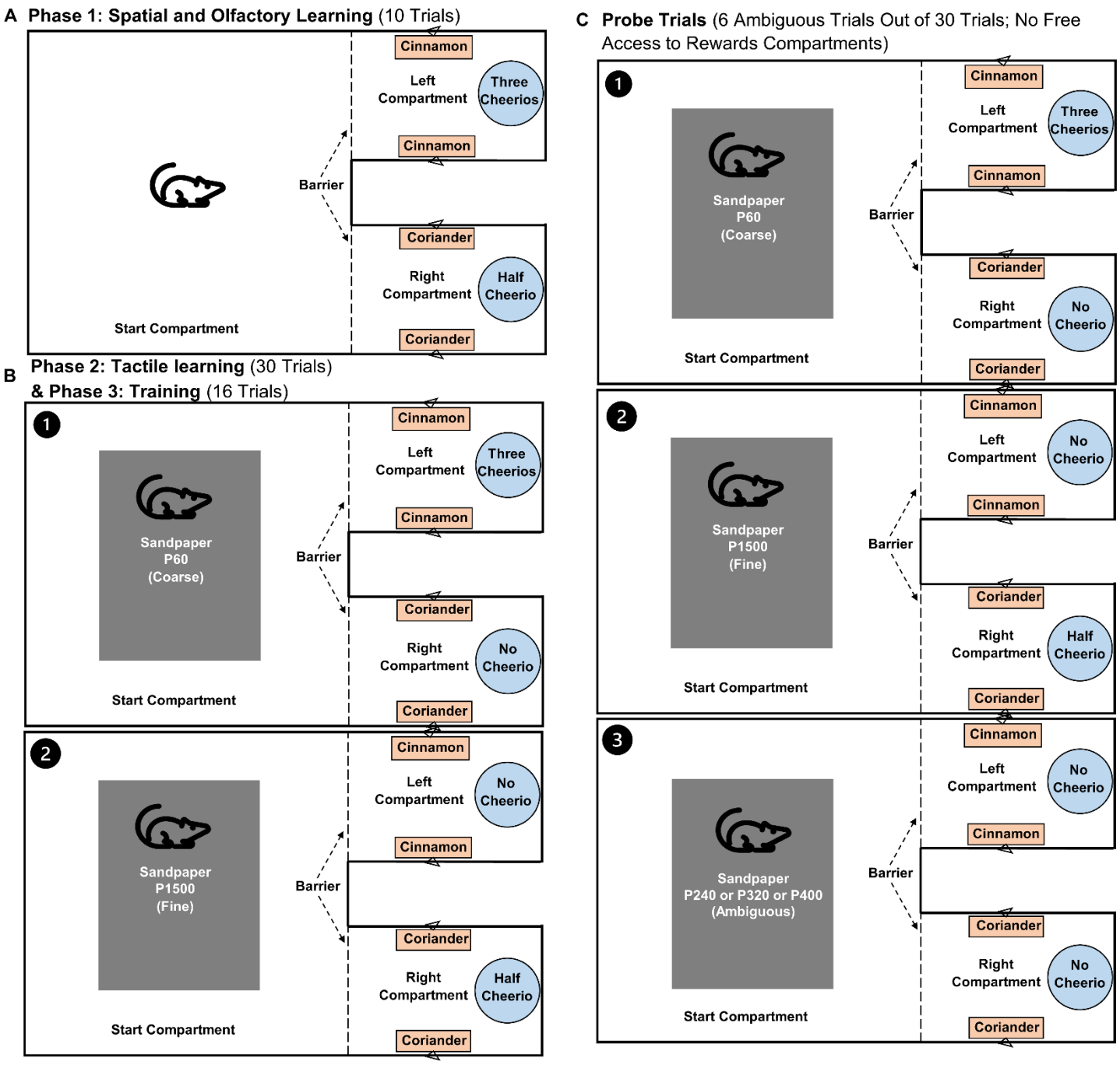

Figure 2. Learning, Training and Probe Protocols. The graph shows the procedure from a rat assigned task combination 1 (*Supplementary Table 1*). **A).** In the spatial and olfactory learning phase, the rat was trained to learn that high reward (three cheerios) was associated with cinnamon scent and left compartment, and low reward (half cheerio) was associated with coriander scent and right compartment; **B).** In the tactile learning phase, the same rat was further trained to learn that fine sandpaper indicated low reward and coarse sandpaper indicated high reward. In the training phase, an acrylic barrier was lowered to block movement between compartments as soon as the rat had made its choice; **C).** In the probe trials, one in every five trials was unrewarded. In these six unrewarded trials, three intermediate and ambiguous grades of sandpaper (P240, P320, P400) were randomly assigned and each presented twice as probes.

initially in the center zone and then allowed to freely explore the arena for ten minutes. The apparatus was wiped with 70% ethanol to remove olfactory cues after each test session. Each session was recorded using a Samsung A70 mobile phone and saved in mp4 format for further

processing and analysis. A total of 52 recordings were acquired at baseline and post-CRS. All original recordings were edited to be ten minutes in duration to remove irrelevant (non-test related) footage. The edited videos were then imported into DeepLabCut (25) to track animal movement by labeling seven body points (*Figure 3A*) and four corners of the testing arena (*Figure 3B*). Main steps involved in the behavioral labelling were: 1). Manually label 11 tracking points of 300 randomly selected video frames (20 frames × 15 videos); 2). Train a deep neural network using labelled frames; 3). Extract the coordinates of all tracking based on the trained network. For each recording, DeepLabCut automatically generated one individual CSV file containing the coordinates of 11 tracking points for all video frames, along with labelling confidence (ranging from 0 ~ 100%) for each coordinate.

All DeepLabCut coordinate files derived from OFT recordings were imported into R 4.4.0. and processed with DLCAnalyzer (26) and in-house R scripts (*Supplementary Scripts*). For each video, the arena outline was first determined by the median coordinates of each corner point using DLCAnalyzer. Also, rat body points with a likelihood below 95% or located outside the testing arena were replaced through data interpolation. Then, the whole arena was virtually divided into a series of 10 x 10 cm blocks based on the arena outline using the in-house script. The outer zone consisted of 16 blocks (in blue, *Figure 3B*), while the inner zone contained 9 blocks (in beige, *Figure 3B*). The percentage of time spent in the outer zone during the first five minutes, second five minutes, and the total ten minutes was computed as a classical measure of anxiety-like behavior.

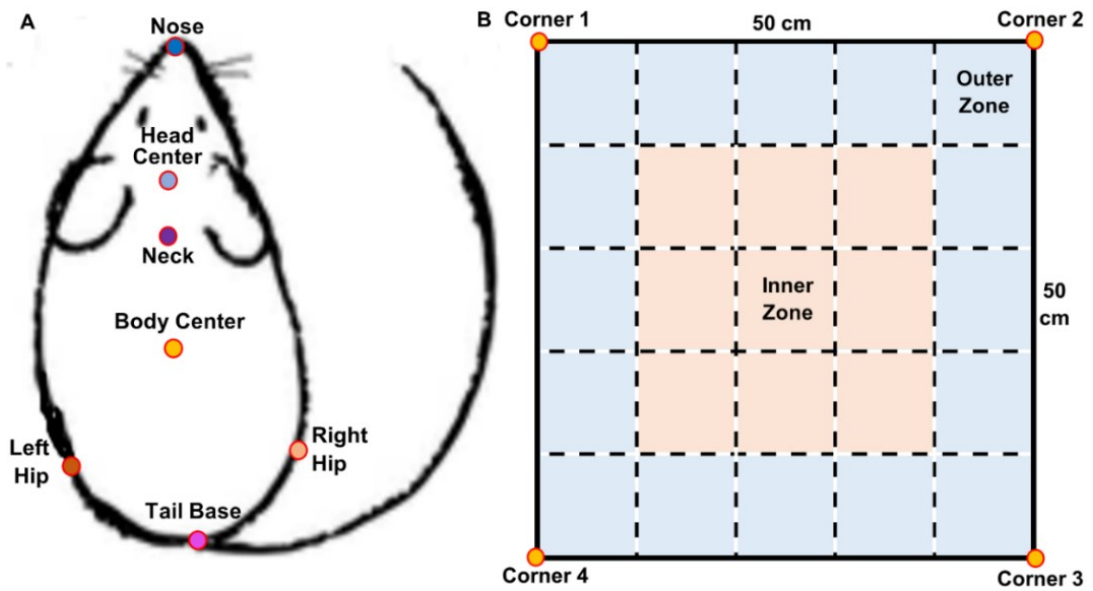

Figure 3. Labels Used to Train the Deep Neural Network. A). Rat with 7 body points; **B).** OFT outline with 4 corners. Beige denotes inner zone. Blue denotes the outer zone.

MRI Acquisition and Batch Processing

Rats were scanned using Bruker Biospec 94/30 US/R pre-clinical MRI machine (Bruker BioSpin GmbH, Germany) operating at 9.4 T (400MHz; H-1). Animals were anesthetized with isoflurane and medetomidine during each MRI session; the anaesthesia protocol was described and

discussed thoroughly in previous work (23, 27). *Supplementary Table 2* summaries the parameters of two scanning sequences: T2w sMRI and rs-fMRI. Both raw images for each scan session were compiled in one ParaVision 6.3.4 package in the format of PvDatasets.

A total of 23 animals completed both baseline and post-CRS scans. One control and one CRS female rat did not complete their baseline scans due to irregular respiratory rate, and one control male's baseline package was corrupted due to technical issues. The batch processing of MRI data followed the same workflow as previous studies (27, 28). The workflow mainly included data organization to the Brain Imaging Data Structure (29), bias field correction, skull stripping, denoising, atlas registration to the Waxholm Space atlas (RRID:SCR_017124; 30), and functional connectivity computation. To compute the functional connectome of the whole brain for each animal, the in-house functional parcellation (28) was mapped onto processed functional images (N = 46) to derive subject-specific time series for 13 functional networks. Fisher's r-to-Z transformation (31) and partial correlation with Tikhonov regularization (default penalty strength of 0.1; 32, 33) was applied to these time series, resulting in 78 ($\frac{13 \times 12}{2}$) network connectivity.

Statistical Analysis

Paired odds ratio (OR) for transition to negative bias from baseline to post-CRS was defined as the ratio of discordant transitions within each sex, using McNemar's matched-pairs framework (34, 35). 95% confidence interval (CI) was computed on the log scale using the standard asymptotic variance for discordant pairs and exponentiated to return to the odds ratio scale. The sex difference in bias shifts was summarized as the ratio of paired odds ratios (ROR), with a log-scale CI calculated by combining the log-scale variances from the sex-specific paired ORs (35).

Behavioural measures and network connectivity were analysed using Linear Mixed-Effects Models (LMMs) using the lme4 package (36) in R. To account for the longitudinal, repeated-measures structure of the data and the dependency within individual animals, models were fitted with the formula: outcome ~ sex * group * timepoint + (1 | animal). This included sex (male vs female), group (CRS vs control), and timepoint (baseline vs post-CRS) as fixed factors and their three-way interaction, with a random intercept for animal to control for repeated-measures variance. Model assumptions, including residual normality and homoscedasticity, were rigorously assessed using the performance package (37). For dependent variables violating these assumptions, a bootstrap method was applied to refit their models (36, 38). Significant three-way interactions were decomposed by assessing simple two-way interactions at each sex-by-group stratum, followed by simple main effects of timepoint, stratified by sex and group. Post-hoc comparisons were conducted using the rstatix (39) R packages, with Bonferroni corrections applied to control for multiple comparisons.

All measurements were presented as mean ± SD, unless otherwise specified. Effect sizes of the analyses were reported with partial eta squared (η^2p) and partial omega squared (ω^2p). Since ω^2p is widely viewed as lesser biased to η^2p, effect sizes were evaluated based on ω^2p and classified into four categories: < 0.02 as very small, 0.02 ~ 0.13 as small, 0.13 ~ 0.26 as medium, and ≥ 0.26

as large (40). Results were considered statistically significant if the p-value was < 0.05 and the effect size was ≥ 0.13.

Correlation between Bias and Network Connectivity

Correlations between bias and network connectivity showing significant two-way interactions were further assessed for each level of sex and group, using a repeated measures correlation approach with the rmcorr R package (41). The repeated measures correlation method yields greater statistical power than conventional correlation approaches, as it is capable of identifying intra-individual associations between variables that may be obscured due to aggregation of data or violation of the independence assumption (41). Results (r_{rm}) were considered statistically significant if the p-value was < 0.05.

Results

Bias Measures

Following CRS, female rats showed higher odds to transit towards a negative bias (paired OR = 3.67, 95% CI: 0.60 ~ 22.30; exact P = 0.22), whereas males showed no directional change (paired OR = 1.00, 95% CI: 0.10 ~ 9.61; exact P = 1.00). The female-to-male ROR was 3.67 (95% CI: 0.20 ~ 66.31), with wide confidence intervals reflecting limited discordant transitions.

For judgement bias, the LMM revealed a significant three-way interaction with a medium effect size among sex, group, and timepoint ($F_{1,22} = 4.95$, $p = 0.037$, $\eta^2p = 0.18$, $\omega^2p = 0.14$). Decomposition via simple two-way interaction analyses showed a significant interaction between group and timepoint with a strong effect size for female rats ($F_{1,10} = 9.20$, $p = 0.013$, $\eta^2p = 0.48$, $\omega^2p = 0.41$), but not in male rats ($F_{1,12} = 0.00$, $p = 1.000$, $\eta^2p = 0.00$, $\omega^2p = 0.00$; *Figure 4A*). Subsequent simple main effects of timepoint within each sex and group stratum were non-significant (*Figure 4B*).

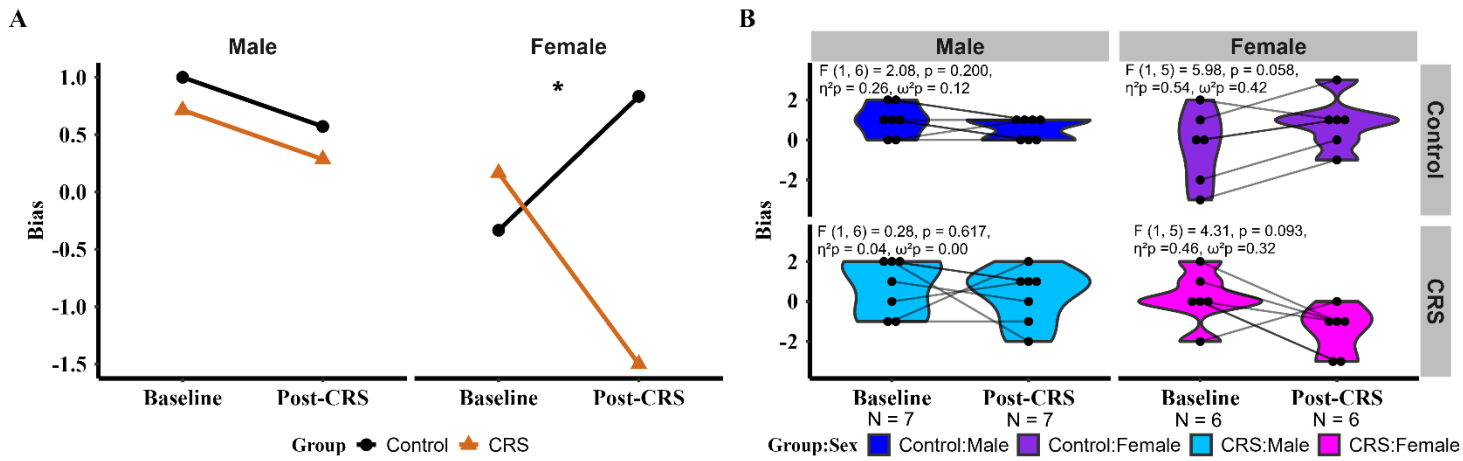

Figure 4. Plots Showing Findings from LMM for Judgement Bias. A). Interaction plot showing the interaction between group and timepoint was significant for female rats, but not for male rats; **B).** Violin plots showing no significant differences in the bias at baseline and post-CRS, for each sex-by-group stratum. Each paired set of observations is connected by a line.

OFT Measures

For all anxiety-like behaviors, LMM models did not identify significant three-way interactions among sex, group, and time (*Supplementary Spreadsheet*). For instance, there was no significant three-way interaction in the total time spent in periphery ($F_{1,22} = 0.09$, $p = 0.76$, $\eta^2p = 0.00$, $\omega^2p = 0.00$).

Network Connectivity

LMM models revealed significant interaction effects for only two out of 78 network connectivity. The remaining 76 measures showed no significant three-way or two-way interactions (*Supplementary Excel*).

For the functional connectivity between left cerebellum-auditory processing and hypothalamus-thalamus network, an LMM revealed a significant three-way interaction with a strong effect size among sex, group, and timepoint ($F_{1,19} = 9.10$, $p = 0.007$, $\eta^2p = 0.32$, $\omega^2p = 0.28$). Further simple two-way interaction analyses for this functional connectivity showed that the interaction between sex and timepoint was significant with a strong effect size for the CRS group ($F_{1,10} = 8.99$, p =

291 0.013, η^2p = 0.47, ω^2p = 0.40), but not for the control group ($F_{1,9}$ = 2.26, p = 0.167, η^2p = 0.20, ω^2p
292 = 0.10; *Figure 5A*). The simple main effect analyses of timepoint further revealed that this network
293 connectivity significantly decreased following two-week CRS with a strong effect size only in
294 female rats ($F_{1,4}$ = 10.51, p = 0.032, η^2p = 0.72, ω^2p = 0.61; *Figure 5B*).
295 Similarly, a significant three-way interaction was found for connectivity between hippocampus-

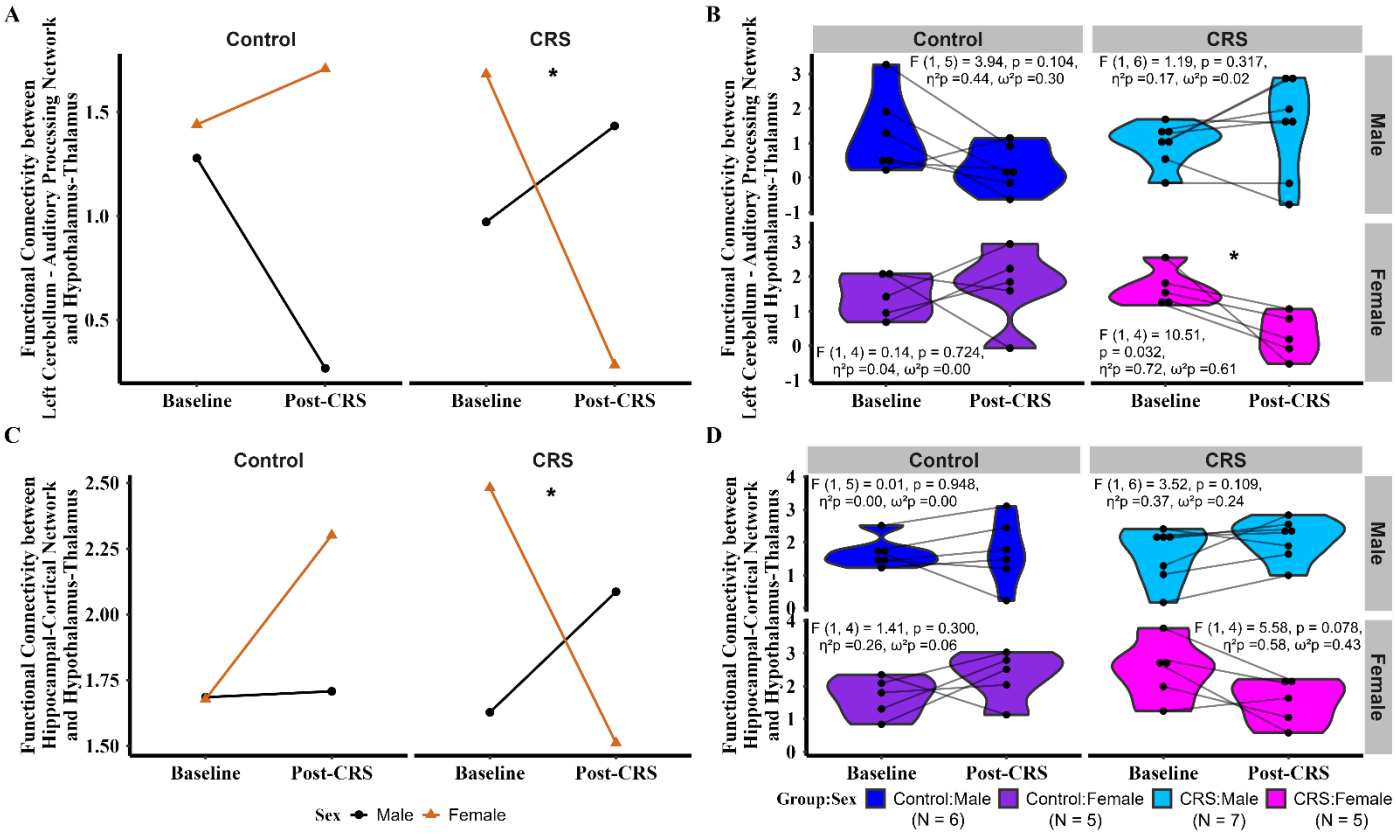

Figure 5. Plots Showing Findings from LMMs for Two Network Connectivity. A). Interaction plot showing the interaction between sex and time was significant in the functional connectivity between left cerebellum-auditory processing network and hypothalamus-thalamus in the control group, but not in the CRS group; **B).** Violin plots showing the connectivity between left cerebellum-auditory processing network and hypothalamus-thalamus significantly decreased following two-week CRS with a strong effect size only in female rats; **C).** Interaction plot showing the interaction between sex and time was significant in the functional connectivity between hippocampus-cortical network and hypothalamus-thalamus for the control group, but for the CRS group; **D).** Violin plots showing no significant differences in the functional connectivity between hippocampus-cortical network and hypothalamus-thalamus at baseline and post-CRS, for each sex-by-group stratum. Each paired set of observations is connected by a line.

296 cortical network and hypothalamus-thalamus among sex, group, and timepoint ($F_{1,19}$ = 7.56, p =
297 0.013, η^2p = 0.28, ω^2p = 0.24). Further simple two-way interaction analyses for this functional
298 connectivity confirmed that the interaction between sex and timepoint was significant within the
299 CRS group ($F_{1,10}$ = 10.12, p = 0.010, η^2p = 0.50, ω^2p = 0.43), whereas the control group showed no
300 interaction ($F_{1,9}$ = 1.02, p = 0.339, η^2p = 0.10, ω^2p = 0.00; *Figure 5C*). However, subsequent simple

main effect analyses of timepoint did not reach significant differences for any specific sex or group stratum (*Figure 5D*).

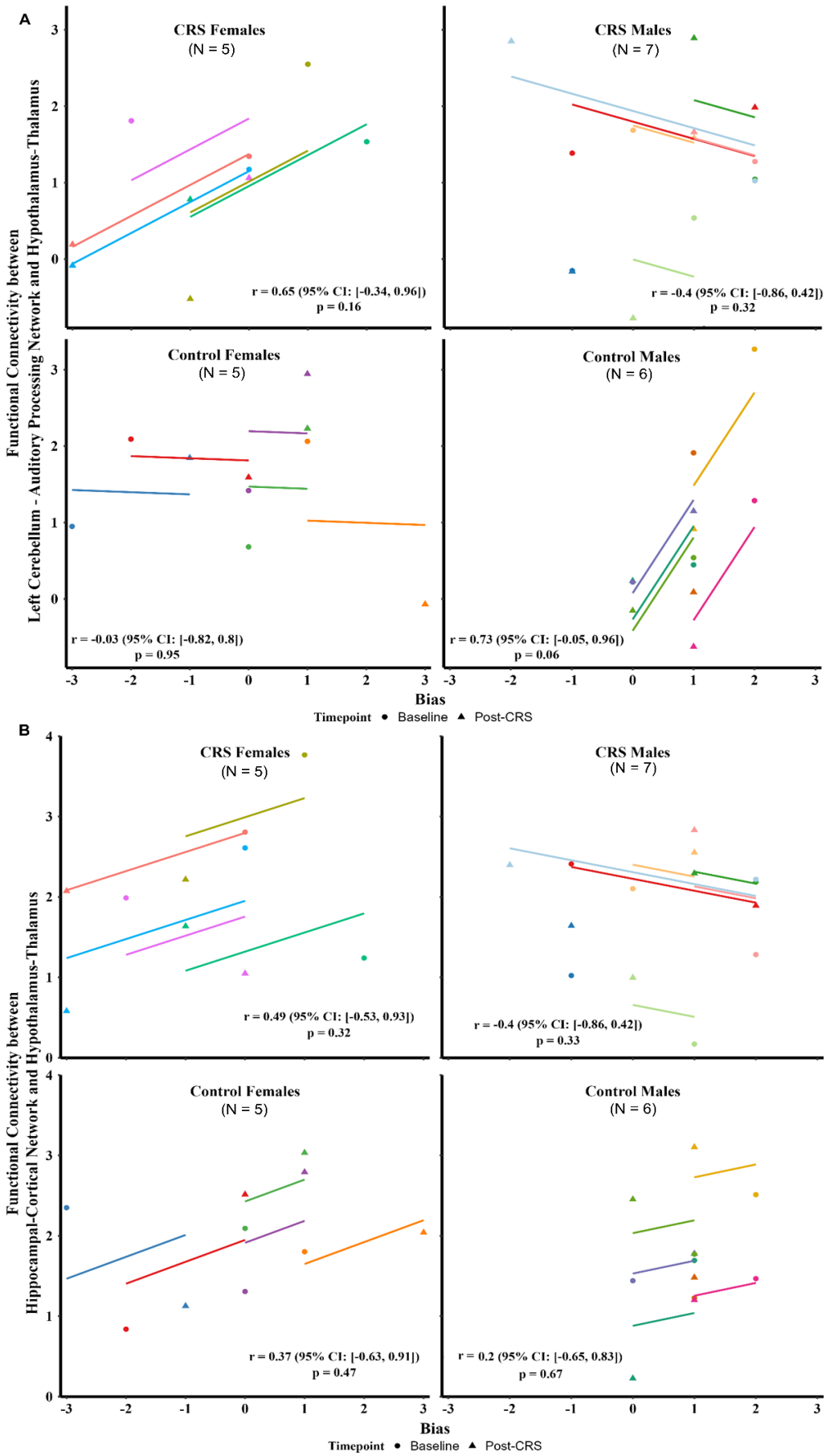

Figure 6. Repeated Measures Correlation Plots. A). Plot showing the repeated-measure correlation between the bias and the functional connectivity between left cerebellum-auditory processing network and hypothalamus-thalamus across sex-by-group strata. **B).** Plot showing the repeated-measure correlation between the bias and the functional connectivity between hippocampus-cortical network and hypothalamus-thalamus across sex-by-group strata. Each animal's data and corresponding correlation line are shown with a different colour.

Correlation between Bias and Network Connectivity

Across sex-by-group strata, repeated-measure correlation between cognitive bias and connectivity in two network pairs described above were not statistically significant ($p > 0.05$, *Figure 6*). However, the intra-individual association showed opposite trends in females and males. Specifically, within the CRS group, females showed moderately positive repeated-measures correlations between bias and network connectivity ($r_{rm} = 0.65$ and 0.49), whereas CRS males showed a weak negative association ($r_{rm} = -0.4$). In the control group, associations were generally weak or absent. Control males were an exception, showing a positive within-individual correlation between bias and functional connectivity between hippocampus-cortical and hypothalamic-thalamic networks ($r_{rm} = 0.73$).

Discussion

The present study aimed to determine whether chronic stress during adolescent produces sex-dependent alterations in cognitive bias and functional connectome in emerging adulthood. A major innovation of the work lies in the longitudinal integration of a translationally relevant judgment bias assay with resting-state connectomes to trace parallel behaviour-network trajectories of stress programming. Following adolescent CRS, adult females showed a greater tendency toward negative bias than males, and a concurrent reduction in functional connectivity between the cerebellum and thalamus. Although repeated-measures correlations between bias and the functional connectivity were not statistically significant, the intra-individual association showed opposite trends in females and males within the CRS group. The results could inform stratified connectome-based interventions targeting adolescent stress exposures to potentially reduce the risk of adult depression.

Sex-Dependent Programming of Negative Cognitive Bias

Negative judgment bias emerging in females following adolescent CRS supports a sex-specific developmental trajectory in cognitive vulnerability. This aligns with evidence that sex differences in depression vulnerability emerge during adolescence (10). One plausible mechanism is sex-dependent programming of the HPA axis during adolescence: repeated glucocorticoid signaling in females may produce enduring changes in stress responsivity that bias appraisal toward pessimism (18). The findings extend work in adult models (42, 43). While adult stress can acutely trigger pessimistic bias (44), these effects are often transient (45). This implies that adult stress may be insufficient to recalibrate cognitive appraisal, whereas adolescence represents a critical period for the programming of adult affective processing (18, 46). These results also broaden the scope of the latent vulnerability framework (47), aligning with convergent human and developmental evidence suggesting that a persistent pessimistic interpretation bias under uncertainty is a sex-dependent recalibration of affective systems, gated by the intersection of sex and developmental timing (48, 49).

Cerebellar-Thalamic Decoupling as a Female-Specific Signature of Stress

The observed shifts in judgment bias were paralleled by a marked decrease in functional connectivity between the left cerebellum-auditory processing and hypothalamus-thalamus network in females. This connectivity disruption aligns with emerging evidence that the cerebellum, beyond its classical motor role, serves as a predictive hub that "tunes" higher-order cognitive and emotional appraisal (50, 51). While neuroimaging studies report direct cerebellum–thalamus hypoconnectivity across the clinical spectrum of depression (52, 53), these cross-sectional data do not account for sex as a moderator, nor determine if decoupling precedes or follows disorder onset. In contrast, the current work demonstrates that adolescent stress triggers cerebellar-thalamic decoupling exclusively in females. Because the judgment bias task requires the precise discrimination of ambiguous tactile cues, such decoupling may compromise the integration of somatosensory information. Specifically, a breakdown in forward models of the cerebellum (54)

may impair the modulation of sensory appraisal under uncertainty, which offers a plausible neural substrate for the persistent pessimistic bias observed in females.

Sex-Specific Dysregulation of the Hippocampal-Hypothalamic Connectivity

The sex-specific impact of adolescent stress extended to the functional connectivity between the hippocampal-cortical network and the hypothalamus. The lack of significant main effect of time suggests that this sex-specific vulnerability is encoded in the trajectory of functional reorganization rather than a single quantum of change in connectivity strength. As the hippocampus provides top-down inhibition of hypothalamic stress circuits (55), this functional decoupling likely represents a failed regulatory gate that facilitates a physiological bias toward negative appraisal of ambiguous environmental cues. While hippocampal–hypothalamic circuits are critical for stress regulation across species (56, 57), the sex-specific consequences in adult of adolescent stress for this functional connectivity have yet to be established.

From Negative Cognitive Bias to Network Decoupling

Several methodological constraints may explain the absence of direct brain-behaviour correlations. First, the anesthetized “resting” state during rs-fMRI captures stable network reorganization, whereas the awake “deciding” brain reflects dynamic cognitive processing (58, 59). Coupled with the two-day separation between assessments, this state and temporal dissociation likely accounts for the lack of correlations. Furthermore, while repeated measure correlations account for intra-individual variance, the study may be underpowered to detect subtle associations. This is particularly relevant for within-group correlations where sample sizes were reduced to less than seven, potentially leading to Type II errors. Despite this, the concurrent of negative bias and reduced cerebellar-thalamic connectivity exclusively within the female CRS group suggests distinct manifestations of a sex-specific "latent trait" of stress vulnerability. However, future investigations should employ multiphoton imaging or electrophysiology to record real-time neural activity during the task (60, 61), directly assessing how circuit dynamics give rise to individual choices under ambiguity.

Conclusion

This study demonstrates that adolescent chronic stress induces enduring, female-specific shifts in judgment bias paralleled by cerebellar-thalamic network reorganization. These findings identify a latent neural architecture of stress programming, demonstrating how adolescent adversity remodels adult affective systems. Such sex-dependent signatures underscore the necessity for stratified, connectome-based interventions to mitigate long-term psychiatric vulnerability.

Acknowledgments

The authors thank Lakshini Piyasiti, Neha Nair, Rebecca Goodyear, and Will Copping for assistance with chronic restraint stress, and UWA Animal Care Services for excellent animal care. The authors also acknowledge the facilities and scientific and technical assistance of the National Imaging Facility, a National Collaborative Research Infrastructure Strategy (NCRIS) capability, at the Centre for Microscopy, Characterisation and Analysis, UWA.

CRediT authorship contribution statement

Twain Dai: Writing - Original Draft, Writing - Review & Editing, Conceptualization, Methodology, Software, Validation, Formal analysis, Investigation, Resources, Data Curation, Visualization**,** Project administration; **Liz Jaeschke-Angi:** Investigation (MRI acquisition)**, Marissa Penrose-Menz:** Investigation (MRI acquisition)**, Tim Rosenow:** Investigation (MRI acquisition)**, Jennifer Rodger:** Conceptualization, Writing - Review & Editing, Supervision**.**

Funding

TD was supported by the Australian Government International Research Training Program scholarship and the Byron Kakulas Prestige scholarship. JR was supported by a program grant from the Stan Perron Charitable Foundation. The funders had no role in study design; data collection, analysis, or interpretation; manuscript preparation; or the decision to submit for publication.

Competing Interests

The authors declare that the research was conducted in the absence of any commercial or financial relationships that could be construed as a potential conflict of interest.

Reference

1. Uddin LQ, Castellanos FX, Menon V. Resting state functional brain connectivity in child and adolescent psychiatry: where are we now? Neuropsychopharmacology (New York, NY). 2024;50(1):196-200.
2. Selemon LD. A role for synaptic plasticity in the adolescent development of executive function. Translational psychiatry. 2013;3(3):e238-e.
3. Sun L, Zhao T, Liang X, Xia M, Li Q, Liao X, et al. Human lifespan changes in the brain's functional connectome. Nature neuroscience. 2025;28(4):891-901.
4. Feng G, Wang Y, Huang W, Chen H, Cheng J, Shu N. Spatial and temporal pattern of structure–function coupling of human brain connectome with development. eLife. 2024;13.
5. Sisk LM, Gee DG. Stress and adolescence: vulnerability and opportunity during a sensitive window of development. Current opinion in psychology. 2022;44:286-92.
6. Rakesh D, Allen NB, Whittle S. Longitudinal changes in within-salience network functional connectivity mediate the relationship between childhood abuse and neglect, and mental health during adolescence. Psychological medicine. 2023;53(4):1552-64.
7. Orchard F, Pass L, Reynolds S. Associations Between Interpretation Bias and Depression in Adolescents. Cognitive therapy and research. 2016;40(4):577-83.
8. Beevers CG, Mullarkey MC, Dainer-Best J, Stewart RA, Labrada J, Allen JJB, et al. Association Between Negative Cognitive Bias and Depression: A Symptom-Level Approach. Journal of abnormal psychology (1965). 2019;128(3):212-27.
9. Vos LMW, Nieto I, Amanvermez Y, Smeets T, Everaert J. Do cognitive biases prospectively predict anxiety and depression? A multi-level meta-analysis of longitudinal studies. Clinical psychology review. 2025;116:102552.
10. Mezulis AH, Funasaki KS, Charbonneau AM, Hyde JS. Gender Differences in the Cognitive Vulnerability-Stress Model of Depression in the Transition to Adolescence. Cognitive therapy and research. 2010;34(6):501-13.
11. Chuang J-Y, Hagan CC, Murray GK, Graham JME, Ooi C, Tait R, et al. Adolescent Major Depressive Disorder: Neuroimaging Evidence of Sex Difference during an Affective Go/No-Go Task. Frontiers in psychiatry. 2017;8:119.
12. Young K, Bellgowan P, Bodurka J, Drevets W. Functional Neuroimaging Correlates of Autobiographical Memory Deficits in Subjects at Risk for Depression. Brain sciences. 2015;5(2):144-64.
13. Lagisz M, Zidar J, Nakagawa S, Neville V, Sorato E, Paul ES, et al. Optimism, pessimism and judgement bias in animals: A systematic review and meta-analysis. Neuroscience and biobehavioral reviews. 2020;118:3-17.
14. Cryan JF, Holmes A. The ascent of mouse: advances in modelling human depression and anxiety. Nature reviews Drug discovery. 2005;4(9):775-90.
15. Borsini A, Giacobbe J, Mandal G, Boldrini M. Acute and long-term effects of adolescence stress exposure on rodent adult hippocampal neurogenesis, cognition, and behaviour. Molecular psychiatry. 2023;28(10):4124-37.
16. McCormick CM, Green MR. From the stressed adolescent to the anxious and depressed adult: Investigations in rodent models. Neuroscience. 2013;249:242-57.
17. Aylward J, Hales C, Robinson E, Robinson OJ. Translating a rodent measure of negative bias into humans: the impact of induced anxiety and unmedicated mood and anxiety disorders. Psychological medicine. 2020;50(2):237-46.
18. Chaby LE, Cavigelli SA, White A, Wang K, Braithwaite VA. Long-term changes in cognitive bias and coping response as a result of chronic unpredictable stress during adolescence. Frontiers in human neuroscience. 2013;7:328.
19. Mengelkoch S, Slavich GM. Sex Differences in Stress Susceptibility as a Key Mechanism Underlying Depression Risk. Current psychiatry reports. 2024;26(4):157-65.
20. Karp NA, Berdoy M, Gray K, Hunt L, Jennings M, Kerton A, et al. The Sex Inclusive Research Framework to address sex bias in preclinical research proposals. Nature communications. 2025;16(1):3763-6.
21. Ghasemi A, Jeddi S, Kashfi K. The laboratory rat: Age and body weight matter. EXCLI journal. 2021;20:1431-45.
22. Brydges NM, Hall L. A shortened protocol for assessing cognitive bias in rats. Journal of Neuroscience Methods. 2017;286:1-5.
23. Seewoo BJ, Hennessy LA, Feindel KW, Etherington SJ, Croarkin PE, Rodger J. Validation of Chronic Restraint Stress Model in Young Adult Rats for the Study of Depression Using Longitudinal Multimodal MR Imaging. eNeuro. 2020;7(4):1-22.
24. Seibenhener ML, Wooten MC. Use of the Open Field Maze to Measure Locomotor and Anxiety-like Behavior in Mice. Journal of visualized experiments. 2015(96):e52434-e.
25. Mathis A, Mamidanna P, Cury KM, Abe T, Murthy VN, Mathis MW, et al. DeepLabCut: markerless pose estimation of user-defined body parts with deep learning. Nature Neuroscience. 2018;21(9):1281-9.

26. Sturman O, von Ziegler L, Schläppi C, Akyol F, Privitera M, Slominski D, et al. Deep learning-based behavioral analysis reaches human accuracy and is capable of outperforming commercial solutions. Neuropsychopharmacology. 2020;45(11):1942-52.
27. Dai T, Seewoo BJ, Hennessy LA, Bolland SJ, Rosenow T, Rodger J. Identifying reproducible resting state networks and functional connectivity alterations following chronic restraint stress in anaesthetized rats. Frontiers in Neuroscience. 2023;17:1151525.
28. Dai T, Algar SD, Small M, Zalesky A, Rodger J. Identifying Neuroimaging Biomarkers of Resilience and Vulnerability to Chronic Stress in An Animal Model: An Exploratory Analysis. bioRxiv. 2025:2025.08.05.667822.
29. Gorgolewski KJ, Auer T, Calhoun VD, Craddock RC, Das S, Duff EP, et al. The brain imaging data structure, a format for organizing and describing outputs of neuroimaging experiments. Scientific Data. 2016;3(1):160044.
30. Papp EA, Leergaard TB, Calabrese E, Johnson GA, Bjaalie JG. Waxholm Space atlas of the Sprague Dawley rat brain. Neuroimage. 2014;97:374-86.
31. Smith SM, Miller KL, Salimi-Khorshidi G, Webster M, Beckmann CF, Nichols TE, et al. Network modelling methods for FMRI. Neuroimage. 2011;54(2):875-91.
32. Liégeois R, Santos A, Matta V, Van De Ville D, Sayed AH. Revisiting correlation-based functional connectivity and its relationship with structural connectivity. Network neuroscience (Cambridge, Mass). 2020;4(4):1235-51.
33. Suri S, Topiwala A, Filippini N, Zsoldos E, Mahmood A, Sexton CE, et al. Distinct resting-state functional connections associated with episodic and visuospatial memory in older adults. NeuroImage (Orlando, Fla). 2017;159:122-30.
34. McNemar Q. Note on the sampling error of the difference between correlated proportions or percentages. Psychometrika. 1947;12(2):153-7.
35. Cleophas TJ, Zwinderman AH. McNemar's Odds Ratios. In: Cleophas TJ, Zwinderman AH, editors. Clinical Data Analysis on a Pocket Calculator: Understanding the Scientific Methods of Statistical Reasoning and Hypothesis Testing. Cham: Springer International Publishing; 2016. p. 275-8.
36. Douglas B, Martin M, Ben B, Steve W. Fitting Linear Mixed-Effects Models Using lme4. Journal of statistical software. 2015;67(1):1-48.
37. Lüdecke D, Ben-Shachar M, Patil I, Waggoner P, Makowski D. performance: An R Package for Assessment, Comparison and Testing of Statistical Models. Journal of open source software. 2021;6(60):3139.
38. Loughin TM. Bootstrap Methods and Their Application. Alexandria: American Statistical Association; 1999. p. 334-5.
39. Kassambara A. rstatix: Pipe-friendly framework for basic statistical tests. CRAN: Contributed Packages. 2019.
40. Cohen J. A Power Primer. Psychological bulletin. 1992;112(1):155-9.
41. Bakdash JZ, Marusich LR. Repeated Measures Correlation. Frontiers in psychology. 2017;8:456.
42. Rygula R, Papciak J, Popik P. Trait Pessimism Predicts Vulnerability to Stress-Induced Anhedonia in Rats. Neuropsychopharmacology (New York, NY). 2013;38(11):2188-96.
43. Papciak J, Popik P, Fuchs E, Rygula R. Chronic psychosocial stress makes rats more 'pessimistic' in the ambiguous-cue interpretation paradigm. Behavioural brain research. 2013;256:305-10.
44. Enkel T, Gholizadeh D, von Bohlen und Halbach O, Sanchis-Segura C, Hurlemann R, Spanagel R, et al. Ambiguous-Cue Interpretation is Biased Under Stress- and Depression-Like States in Rats. Neuropsychopharmacology (New York, NY). 2010;35(4):1008-15.
45. Aliphon B, Dai T, Moretti J, Penrose-Menz M, Mulders WHAM, Blache D, et al. A repeated measures cognitive affective bias test in rats: comparison with forced swim test. Psychopharmacology. 2022.
46. Avital A, Richter-Levin G. Exposure to juvenile stress exacerbates the behavioural consequences of exposure to stress in the adult rat. The international journal of neuropsychopharmacology. 2005;8(2):163-73.
47. McCrory EJ, Viding E. The theory of latent vulnerability: Reconceptualizing the link between childhood maltreatment and psychiatric disorder. Development and psychopathology. 2015;27(2):493-505.
48. Nweze T, Ezenwa M, Ajaelu C, Hanson JL, Okoye C. Cognitive variations following exposure to childhood adversity: evidence from a pre-registered, longitudinal study. EClinicalMedicine. 2023;56:101784-.
49. Ho TC, Buthmann J, Chahal R, Miller JG, Gotlib IH. Exploring sex differences in trajectories of pubertal development and mental health following early adversity. Psychoneuroendocrinology. 2024;161:106944-.
50. Malatesta G, D'Anselmo A, Prete G, Lucafò C, Faieta L, Tommasi L. The Predictive Role of the Posterior Cerebellum in the Processing of Dynamic Emotions. Cerebellum (London, England). 2024;23(2):545-53.
51. Manto M, Adamaszek M, Apps R, Carlson E, Guarque-Chabrera J, Heleven E, et al. Consensus Paper: Cerebellum and Reward. Cerebellum (London, England). 2024;23(5):2169-92.

52. Chen Y, Wang C, Zhu X, Tan Y, Zhong Y. Aberrant connectivity within the default mode network in first-episode, treatment-naïve major depressive disorder. Journal of affective disorders. 2015;183:49-56.
53. Tu P-C, Chang W-C, Su T-P, Lin W-C, Li C-T, Bai Y-M, et al. Thalamocortical functional connectivity and rapid antidepressant and antisuicidal effects of low-dose ketamine infusion among patients with treatment-resistant depression. Molecular Psychiatry. 2025;30(1):61-8.
54. Welniarz Q, Worbe Y, Gallea C. The Forward Model: A Unifying Theory for the Role of the Cerebellum in Motor Control and Sense of Agency. Frontiers in systems neuroscience. 2021;15:644059.
55. Cole AB, Montgomery K, Bale TL, Thompson SM. What the hippocampus tells the HPA axis: Hippocampal output attenuates acute stress responses via disynaptic inhibition of CRF+ PVN neurons. Neurobiology of stress. 2022;20:100473.
56. Goldfarb EV, Rosenberg MD, Seo D, Constable RT, Sinha R. Hippocampal seed connectome-based modeling predicts the feeling of stress. Nature communications. 2020;11(1):2650-10.
57. Bang JY, Zhao J, Rahman M, St-Cyr S, McGowan PO, Kim JC. Hippocampus-Anterior Hypothalamic Circuit Modulates Stress-Induced Endocrine and Behavioral Response. Frontiers in neural circuits. 2022;16:894722.
58. Tauber JM, Brincat SL, Stephen EP, Donoghue JA, Kozachkov L, Brown EN, et al. Propofol-mediated Unconsciousness Disrupts Progression of Sensory Signals through the Cortical Hierarchy. Journal of cognitive neuroscience. 2024;36(2):394-413.
59. Bonhomme V, Staquet C, Montupil J, Defresne A, Kirsch M, Martial C, et al. General Anesthesia: A Probe to Explore Consciousness. Frontiers in systems neuroscience. 2019;13:36.
60. Vickers ED, McCormick DA. Pan-cortical 2-photon mesoscopic imaging and neurobehavioral alignment in awake, behaving mice. eLife. 2024;13.
61. Steinmetz NA, Aydin C, Lebedeva A, Okun M, Pachitariu M, Bauza M, et al. Neuropixels 2.0: A miniaturized high-density probe for stable, long-term brain recordings. Science (American Association for the Advancement of Science). 2021;372(6539).

555 # Figure legends

Figure 1. Study Design and Timeline. All animals were habituated to the new environment for nine days after their arrival and prior to experiments. All rats were trained on JBT, for up to nine days. Behavioural tests and MRI scan were conducted before and after 14 consecutive days of CRS.

Figure 2. Learning, Training and Probe Protocols. The graph shows the procedure from a rat assigned task combination 1 (*Supplementary Table 1*). **A).** In the spatial and olfactory learning phase, the rat was trained to learn that high reward (three cheerios) was associated with cinnamon scent and left compartment, and low reward (half cheerio) was associated with coriander scent and right compartment; **B).** In the tactile learning phase, the same rat was further trained to learn that fine sandpaper indicated low reward and coarse sandpaper indicated high reward. In the training phase, an acrylic barrier was lowered to block movement between compartments as soon as the rat had made its choice; **C).** In the probe trials, one in every five trials was unrewarded. In these six unrewarded trials, three intermediate and ambiguous grades of sandpaper (P240, P320, P400) were randomly assigned and each presented twice as probes.

Figure 3. Labels Used to Train the Deep Neural Network. A). Rat with 7 body points; **B).** OFT outline with 4 corners. Beige denotes inner zone. Blue denotes the outer zone.

Figure 4. Plots Showing Findings from LMM for Judgement Bias. A). Interaction plot showing the interaction between group and timepoint was significant for female rats, but not for male rats; **B).** Violin plots showing no significant differences in the bias at baseline and post-CRS, for each sex-by-group stratum. Each paired set of observations is connected by a line.

Figure 5. Plots Showing Findings from LMMs for Two Network Connectivity. A). Interaction plot showing the interaction between sex and time was significant in the functional connectivity between left cerebellum-auditory processing network and hypothalamus-thalamus in the control group, but not in the CRS group; **B).** Violin plots showing the connectivity between left cerebellum-auditory processing network and hypothalamus-thalamus significantly decreased following two-week CRS with a strong effect size only in female rats; **C).** Interaction plot showing the interaction between sex and time was significant in the functional connectivity between hippocampus-cortical network and hypothalamus-thalamus for the control group, but for the CRS group; **D).** Violin plots showing no significant differences in the functional connectivity between hippocampus-cortical network and hypothalamus-thalamus at baseline and post-CRS, for each sex-by-group stratum. Each paired set of observations is connected by a line.

Figure 6. Repeated Measures Correlation Plots. A). Plot showing the repeated-measure correlation between the bias and the functional connectivity between left cerebellum-auditory processing network and hypothalamus-thalamus across sex-by-group strata. **B).** Plot showing the repeated-measure correlation between the bias and the functional connectivity between hippocampus-cortical network and hypothalamus-thalamus across sex-by-group strata. Each animal's data and corresponding correlation line are shown with a different colour.